IEEE Access
Multidisciplinary | Rapid Review | Open Access Journal

Received 21 November 2023, accepted 3 December 2023, date of publication 5 December 2023,
date of current version 13 December 2023.

Digital Object Identifier 10.1109/ACCESS.2023.3339879

RESEARCH ARTICLE

Modeling and Hybrid PSO-WOA-Based Intelligent PID and State-Feedback Control for Ball and Beam Systems

NUR SYAZREEN AHMAD, (Member, IEEE)
School of Electrical and Electronic Engineering, Universiti Sains Malaysia, Nibong Tebal, Penang 14300, Malaysia
e-mail: syazreen@usm.my

This work was supported by Ministry of Higher Education, Malaysia for Fundamental Research Grant Scheme with Project Code: FRGS/1/2021/TK0/USM/02/18.

ABSTRACT The ball and beam (BnB) system serves as a benchmark in control engineering as it provides a foundational concept applicable to addressing stabilization challenges of various underactuated nonlinear systems. This includes tasks like maintaining the balance of goods carried by mobile robots and controlling the attitude of unmanned aerial vehicles. In this study, the focus is on enhancing control optimization strategies for BnB systems that take into account inherent nonlinearities arising from actuator constraints and state measurements. The work introduces a novel intelligent control approach, termed hybrid PSO-WOA, which combines Particle Swarm Optimization (PSO) and Whale Optimization Algorithm (WOA) to automate optimal parameter search for proportional-integral-derivative (PID) and state feedback (SF) controllers. The collaborative technique between PSO and WOA is formulated to strike a balance between exploration and exploitation phases, and to mitigate premature convergence risks due to the system's complexities. Additionally, three control schemes, namely cascade PID-PID, cascade PID-SF, and cascade PID-observer are introduced, each with tailored cost functions for optimization through the hybrid PSO-WOA algorithm, accommodating both measurable and unmeasurable state scenarios. Simulation results consistently demonstrate the superior performance of the hybrid approach compared to individual PSO and WOA methods, as well as conventional PID and linear quadratic regulator approaches. Notably, the hybrid approach exhibits a significant improvement in error metrics, reducing integral-time absolute error by 18.99%, integral squared error by 35.37%, and steady-state error by 92.86%. This substantial enhancement suggests promising directions for future research in automated control parameter tuning for underactuated nonlinear systems.

INDEX TERMS Ball and beam, feedback control, hybrid, intelligent control, particle swarm optimization, proportional-integral-derivative, whale optimization algorithm.

I. INTRODUCTION

The ball and beam (BnB) system emerges as an exceptional framework for evaluating and refining control strategies, particularly tailored for stabilization of nonlinear dynamical systems. The system's inherent complexity, driven by factors such as saturation characteristics of its actuators, constraints posed by the direct current (DC) motor, and discontinuities in position measurements, mirrors the real-world challenges commonly faced in underactuated nonlinear systems [1]. Designing controls for such systems presents substantial challenges due to their unpredictable and dynamic characteristics [2], [3]. Practical applications of the BnB system include robotic load balancing [4], [5], [6], [7], attitude control in space vehicles [8], [9], nonlinear control of actuators [10], and gyroscopic stabilization systems [11]. This versatility allows researchers to leverage the BnB system for designing, implementing, and testing control algorithms

The associate editor coordinating the review of this manuscript and approving it for publication was Xiong Luo.

capable of navigating through nonlinear dynamics and stabilizing the system despite its underactuated nature. The broad spectrum of potential applications provides a valuable opportunity to assess the adaptability and transferability of control methodologies across various contexts [12].

The primary objective of the BnB system is to stabilize the ball at the equilibrium position by controlling the beam motion and maintaining its stability in the presence of external disturbances. Nonetheless, formulating a robust controller poses a significant challenge due to the aforementioned complexities. Traditionally, a common solution to the ball-position stabilization problem has been the adoption of a proportional-derivative (PD) regulator with position error. This choice is based on the need to address the double integral dynamics following the linearization of nonlinear dynamics near the operating point. An advanced two degrees-of-freedom fractional control technique is introduced in [13] through experimental comparisons between integer and fractional order controls, which can be considered as an improved version of the PD controller. However, PD control may encounter a steady-state error caused by unmodeled dynamics and external forces. To address this, an integral action is typically incorporated into the control law to form a proportional-integral-derivative (PID) controller.

Alternative methods include state-space approaches such as state-feedback with pole-placement [14], observer-based compensator [15], and linear quadratic regulator (LQR) [16]. These controllers are typically cascaded to ensure stability of each actuator in the BnB system. H_2 and H_∞ techniques are other modern control approaches that can be used to stabilize the BnB [17], [18], but these approaches typically require precise system parameter information and several loop transformations to convexify the parameter search [19]. A more advanced technique is presented in [20] and [21] where an active disturbance rejection control is employed to enhance the balancing performance of BnB systems by accurately tracking the ball position and DC motor. This approach however necessitates the utilization of sophisticated tools and hardware, potentially limiting its applicability to smaller or less complex control systems. Previous studies have also explored the use of nonlinear controllers such as neural networks [22], [23], [24], [25], fuzzy logic [26], [27], [28], [29], backstepping [30], deep reinforcement learning [31], and passivity-based control [32], as alternative strategies for stabilizing the BnB system.

Despite the availability of various control techniques for stabilizing BnB systems, PID and state feedback (SF) or LQR are often preferred due to their simplicity and robustness against parameter variations [33], [34], [35], [36], [37]. In [38] for instance, it has been demonstrated via MATLAB simulation that a cascade PID control outperforms a neural-network-based compensator in terms of overshoot and error. Recent works have also focused on enhancing the tuning strategies for these controllers by employing evolutionary algorithms [39], [40], [41]. For instance, in works such as [42] and [43], controller performance is improved through the application of a genetic algorithm (GA) for parameter tuning. Alternative parameter optimization methods include particle swarm optimization (PSO), artificial bee colony (ABC) and bat algorithm (BA) [44]. The research conducted by Coskun et al. [45] highlights a substantial performance enhancement of PSO-optimized PID controllers compared to the conventional PID approach when implemented in an industrial electro-hydraulic system. In the study by Ouyang et al. [46], it was observed that PSO exhibits faster convergence toward optimal solutions compared to GA in PID parameter tuning. It has also been demonstrated in [47] that PSO-optimized PID controllers outperform those optimized through ABC and BA. Additionally, the studies in [48] and [49] have demonstrated performance improvements in PID control when optimized through the Whale Optimization Algorithm (WOA) compared to conventional approaches. Recent findings in [50] have also highlighted the superiority of WOA-optimized PID controllers over those optimized through PSO and Grey Wolf Optimization (GWO).

Employing the evolutionary algorithms to optimize the controllers nonetheless can be challenging when the nonlinearities are incorporated into the model as local minima issue is bound to occur, which consequently leads to suboptimal values [51]. One way to improve the algorithm is through hybridization, which involves combining different methods [52], [53], [54]. As an illustration, in [55], a hybridization of PSO with WOA was introduced, employing PSO during the exploration phase and WOA during the exploitation phase. This strategy showcased improved performance compared to both PSO and WOA across several unconstrained optimization problems. However, given the underactuated and highly nonlinear nature of the BnB system, it is crucial to carefully tailor the collaboration technique between different algorithms to mitigate the risk of being trapped in local minima during optimization.

Apart from optimizing control parameters, the configuration of controllers and restrictions on state measurements can significantly impact the performance of the closed-loop system. While each control configuration comes with its advantages, the choice typically depends on factors such as the system's structure, prior understanding of the system's model, the hardware in use, and the feasibility of obtaining state measurements [56], [57]. For instance, a cascade PID compensator is particularly well-suited for situations where it is impossible to measure certain state variables. Conversely, in situations where the state variables can be measured, employing the state-space approach offers a systematic and unified framework for modeling and analyzing the system's dynamics, thus facilitating control design [58], [59]. In instances where controlling the states is preferable but adding extra sensors is impractical due to cost or space limitations, observers can be employed to estimate the state variables. Nonetheless, altering control configurations introduces changes to the complexity of the control design, and necessitates a different fine-tuning method and a reassessment of both closed-loop stability and performance.

In this study, the focus is on enhancing the control optimization strategy for both measurable and unmeasurable state conditions in BnB systems which take into account the inherent nonlinearities arising from the constraints of the actuators and state measurements. The contributions of this paper are outlined as follows

- a novel intelligent control approach is proposed which combines PSO and WOA, referred to as hybrid PSO-WOA, to automate the search for optimal control parameters for the nonlinear BnB system that is modeled based on Newton's laws of motion. This method can bypass the need for meticulous fine-tuning design processes that usually demand prior expertise
- a new collaboration technique between PSO and WOA that seeks to strike a balance between the exploration and exploitation phases, thereby mitigating the risk of premature convergence that is bound to occur due to the complexity of the nonlinear BnB system
- development of three distinct control schemes for the nonlinear BnB system, namely cascade PID-PID, cascade PID-SF, and cascade PID-observer. Each of these schemes is equipped with suitable cost functions for optimization through the hybrid PSO-WOA algorithm, catering to both measurable and unmeasurable state scenarios

The effectiveness of the proposed optimization algorithm is validated through extensive MATLAB simulations involving the three control feedback configurations, each requiring a distinct search space dimension. Results demonstrate that the proposed hybrid PSO-WOA approach consistently outperforms both PSO and WOA individually, as well as conventional PID and LQR methods. Furthermore, this superior performance remains consistent across different scenarios and feedback configurations, highlighting the generalizability of the approach.

The subsequent sections of the paper are organized as follows: Section II introduces the BnB modeling method, outlines the formulation of the hybrid PSO-WOA algorithm, and presents the proposed control schemes along with the corresponding cost functions. Section III showcases and analyzes the simulation results, while Section IV summarizes the findings and provides suggestions for future work.

II. METHODOLOGY

A. BALL AND BEAM MODELING

The depicted BnB system in Fig. 1 aims to regulate the position of the ball, represented by the red circle, and ensure it reaches and remains stable at $x = 0$ by adjusting the beam's angle which is controlled by a DC motor. The system's parameters are specified in Table 1. The assumptions made for the BnB system are as follows:

(i) The ball encounters friction, possesses a rotary moment of inertia, and undergoes acceleration as it moves along the beam
(ii) The beam angle, θ, is small
(iii) Both the masses of the ball and the beam are uniformly distributed
(iv) The ball maintains contact with the beam and the rolling occurs without slipping

Taking x as the position of the ball on the beam with respect to the origin, the ball's velocity and acceleration can be written as

$$\dot{x} = \frac{dx}{dt}, \quad \text{and} \quad \ddot{x} = \frac{d^2x}{dt^2} \tag{1}$$

respectively. The motion of the ball is influenced by two forces: F_{tx} and F_{rx}. These forces represent the effects of the ball's translational and rotational motion, respectively. Specifically, F_{tx} can be described as $F_{tx} = m\ddot{x}$. To determine F_{rx}, we can use the equation $T_r = F_{rx}r$, where T_r represents the torque resulting from the ball's rotation. However, since

$$T_r = J_b\frac{d\omega_b}{dt} = J_b\frac{d(\frac{v_b}{r})}{dt} = \frac{J_b}{r}\frac{d}{dt}(\frac{dx}{dt}) = \frac{J_b}{r}\ddot{x} \tag{2}$$

where ω_b is the ball's rotational speed, and v_b is the ball's translational speed, we will get

$$F_{rx} = \frac{J_b}{r^2}\ddot{x}. \tag{3}$$

Based on Newton's second law, we can write

$$mg\sin\theta - F_{rx} = F_{tx}, \quad mg\sin\theta - \frac{J_b}{r^2}\ddot{x} = m\ddot{x}. \tag{4}$$

Via small angle approximation, i.e. $\sin\theta \approx \theta$, we will obtain

$$mg\theta = (\frac{J_b}{r^2} + m)\ddot{x} \tag{5}$$

$$\ddot{x} = \Big(\frac{mg}{J_b/r^2 + m}\Big)\theta. \tag{6}$$

Applying the Laplace transform (assuming zero initial condition) on (6) gives us $s^2X(s) = \Big(\frac{mg}{J_b/r^2 + m}\Big)\theta(s)$, or equivalently,

$$\frac{X(s)}{\theta(s)} = \frac{1}{s^2}\Big(\frac{mg}{J_b/r^2 + m}\Big) \tag{7}$$

which is the transfer function from θ to x. As the DC motor is used to control the beam, it is essential to derive the transfer function relating to the DC motor angular displacement, i.e. α, to the ball position, x. Since the relationship between θ and α is simply $\theta = \gamma_0\alpha$ where γ_0 is just a constant gain that can be obtained via experiment, we can rewrite (7) as follows:

$$\frac{X(s)}{\alpha(s)} = \frac{\gamma_0}{s^2}\Big(\frac{mg}{J_b/r^2 + m}\Big) \tag{8}$$

or, equivalently.

$$s^2X(s) = \gamma_0\alpha(s)\Big(\frac{mg}{J_b/r^2 + m}\Big). \tag{9}$$

In the state-space domain, we will get

$$\ddot{x} = \gamma_0\alpha Q_b \quad \text{where} \quad Q_b = \Big(\frac{mg}{J_b/r^2 + m}\Big) \tag{10}$$

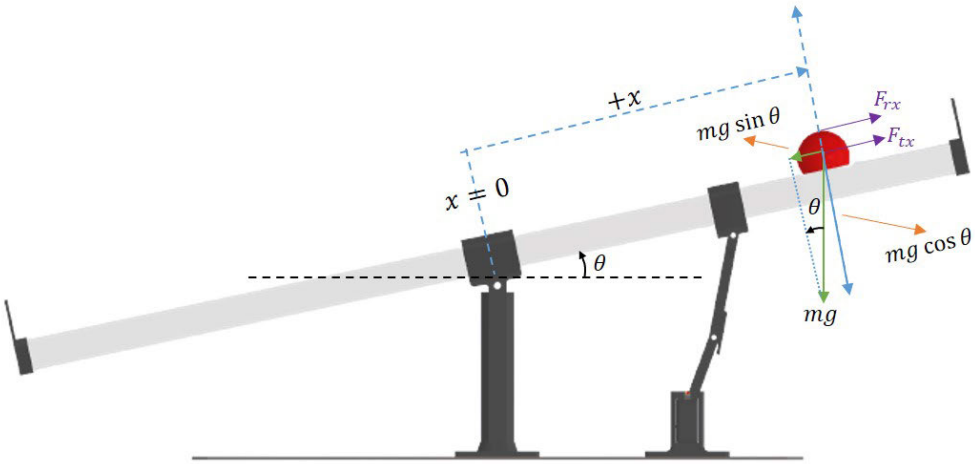

FIGURE 1. Ball and beam.

Hence

$$\begin{bmatrix}\dot{x}\\ \ddot{x}\end{bmatrix}=\begin{bmatrix}0 & 1\\ 0 & 0\end{bmatrix}\begin{bmatrix}x\\ \dot{x}\end{bmatrix}+\begin{bmatrix}0\\ \gamma_0 Q_b\end{bmatrix}\alpha,\quad x=\begin{bmatrix}1 & 0\end{bmatrix}\begin{bmatrix}x\\ \dot{x}\end{bmatrix} \tag{11}$$

Since $J_b = (2/5)mr^2$, it follows that $Q_b = \frac{5g}{7}$. By writing the state variables as $x_1 = x$ and $x_2 = \dot{x}$, the state space representation of the BnB system can be written as

$$\begin{bmatrix}\dot{x}_1\\ \dot{x}_2\end{bmatrix}=\begin{bmatrix}0 & 1\\ 0 & 0\end{bmatrix}\begin{bmatrix}x_1\\ x_2\end{bmatrix}+\begin{bmatrix}0\\ \gamma\end{bmatrix}\alpha,\quad y=\begin{bmatrix}1 & 0\end{bmatrix}\begin{bmatrix}x_1\\ x_2\end{bmatrix} \tag{12}$$

where $\gamma = (5/7)g\gamma_0$. With regard to the DC motor, the corresponding model can be derived based on the following equations:

$$\begin{cases} T_m = K_t i \\ T_m = J_m\ddot{\alpha} + T_{load} \\ V_b = K_v\dot{\alpha} \\ V_s = L_m\dfrac{di}{dt} + R_m i + V_b \end{cases} \tag{13}$$

where T_m is the motor torque, K_t is the torque constant, i is the armature current, J_m is the motor inertia, T_{load} is the load torque, V_s is the voltage supply, V_b is the back-electromotive force (EMF), K_v is the back-EMF constant, $\dot{\alpha}$ is the angular velocity, and R_m and L_m are armature-equivalent resistor and inductor respectively. Usually the motor torque constant and back-EMF constant share the same value, i.e. $K_t \approx K_v$. To simplify, let K_m represent K_t and K_v, and assume L_m and T_{load} to be negligibly small. With some rearrangements in the previous equations, the transfer function from the voltage supply, V_s, to the motor's angular displacement,α, can be established as follows

$$G_m(s) = \frac{K_m}{J_m R_m s + K_m^2}\left(\frac{1}{s}\right) \tag{14}$$

TABLE 1. Ball and beam parameters.

Parameter	Description	Value/Unit
L	Beam length	1.0 m
m	Mass of the ball	0.014 kg
r	Radius of the ball	0.0185 m
J_b	Ball's moment of inertia	$(2/5)\text{mr}^2$ kgm^2
g	Gravitational acceleration	9.8 ms^{-2}
F_{tx}	Force due to translational motion	kg ms^{-2}
F_{rx}	Force due to ball rotation	kg ms^{-2}
θ	Beam angle	rad
x	Ball position	$\pm$0.4 m
γ_0	constant gain	0.924
K_m	motor torque/back-emf constant	$14.7e^{-3}$ V/(rads^{-1})
J_m	DC motor's inertia	$42.6e^{-6}$ kgm^2
R_m	armature-equivalent resistor	4.67Ω
α	DC motor angular displacement	$\pm$0.175 rad

B. PARTICLE SWARM OPTIMIZATION (PSO)

PSO is a computer algorithm inspired by how animals like fish and birds work together. It was invented in 1995 by Eberhart and Kennedy [60], and it is widely used in engineering and science to solve various problems. Within the PSO framework, each particle embodies a point within a search space of D dimensions. The term ''swarm'' denotes the assembly of particles present during a particular iteration, collectively navigating the space with a specific velocity. During the search process, the position of the i-th particle, denoted as $P_i(k)$, evolves through updates aiming to approach the global optimum. These updates are guided by the particle's velocity vector, represented as $V_i(k)$. The velocity vector of the i-th particle undergoes modification at the k-th iteration grounded on the following two factors:

1) The historical best position of the i-th particle, referred to as the local best particle (pbest), and denoted as $P_{bi}(k)$, and

2) The historical best position attained by the entire swarm, known as the global best particle (gbest), and denoted as $g_b(k)$.

The i-th particle's velocity and position will then be updated as follows:

$$V_i(k+1) = wV_i(k) + c_1 r_1(P_{bi}(k) - P_i(k)) + c_2 r_2(g_b(k) - P_i(k)) \quad (15)$$

$$P_i(k+1) = P_i(k) + V_i(k+1) \quad (16)$$

where $w \in [0, 1]$ is the inertia weight that determines how much a particle maintains its prior velocity.; c_1 and c_2 are the cognitive and the social parameters respectively; and r_1, r_2 represent two uniformly distributed random numbers between 0 and 1. The velocity equation comprises three distinct parts, i.e. inertia, cognitive, and social terms, which are represented by $wV_i(k)$, $c_1 r_1(P_{bi}(k) - P_i(k))$, and $c_2 r_2(g_b(k) - P_i(k))$ respectively. The inertia term ensures a level of consistency in particle velocity between iterations. The cognitive term steers the particle towards its best-known position, aiming to improve upon past performance. The social term guides the particle towards the best position within its neighborhood. These three components each contribute uniquely to the optimization process. The inertia component encourages broad exploration of the search space. On the other hand, the cognitive and social components collaborate to focus the search on promising solutions found up to the current iteration. This synergy between components enables PSO to strike a balance between exploration and exploitation, ultimately aiding in the optimization of complex problems.

Algorithm 1 Pseudo-Code of the Standard PSO

```
for i = 1, ..., n do
    Randomly initialize P_i
    Randomly initialize V_i (or set to 0)
    Set the constants w, c_1, c_2, r_1, r_2
    Set P_bi = P_i
end for
while k ≤ k_max do
    for i = 1, ..., N do
        Evaluate the fitness of particle i, f(P_i)
        if f(P_bi(k)) ≥ f(P_bi(k−1)) then P_bi(k) = P_bi(k−1)
        else
            P_bi(k) = P_i(k)
        end if
        g_b(k) = min{f(P_b0(k)), f(P_b1(k)), ..., f(P_bn(k))}
        Update V_i(k + 1) according to (15)
        Update P_i(k + 1) according to (16)
    end for
    k++
end while
```

C. WHALE OPTIMIZATION ALGORITHM (WOA)

In the context of WOA, the simulation involves emulating the actions of humpback whales, which exhibit a specific behavior called "bubble-net foraging" wherein they adopt a spiral trajectory around their prey and then transition into a tightening circular path when launching an attack [61]. The whales' actions linked to bubbles are identified and labeled as 'upward-spirals' and 'double-loops'. As depicted in Fig. 2, the bubbles created by whales create a path that obstructs the movement of fish. Over time, the circular shape (spirals) reduces in size (radius), eventually leading to the aggregation of fish in a single location.

During hunting, humpback whales often encircle their prey. The WOA technique assumes that the current best solution is similar to the desired outcome or is very close to the optimal point because the exact location of the best solution in the search space is not known beforehand. The rest of the search agents then aim to reposition themselves closer to the leading search agent once it has been identified. This behavior is illustrated by the following equations

$$\begin{cases} \overrightarrow{S}(k+1) = \overrightarrow{S}^*(k) - \overrightarrow{A} \cdot \overrightarrow{D} \\ \overrightarrow{A} = 2\vec{a}\vec{r}_1 - \vec{a}, \quad \vec{a} = 2 - 2(k/k_{max}) \\ \overrightarrow{D} = |\overrightarrow{C} \cdot \overrightarrow{S}^*(k) - \overrightarrow{S}(k)|, \quad \overrightarrow{C} = 2\vec{r}_2 \end{cases} \quad (17)$$

where $\overrightarrow{S}$ denotes the vector representing the current whale's position, $\overrightarrow{S}^*$ denotes the values of the best whale in the population, $\overrightarrow{r}_1$, $\overrightarrow{r}_2$ are random vectors in the [0, 1] range, and a is a parameter that linearly decreases from 2 to 0, functioning as the distance control factor.

During the bubble-net attacking phase, two distinct behaviors become apparent. The first involves a shrinking encircling mechanism, characterized by a diminishing hunting circle. The second behavior is related to spiral position updates, where the separation between the whale and the prey is adjusted. The whales exhibit a simultaneous swimming behavior where they spiral around their prey while also narrowing their circular movement. To replicate this concurrent action, it is assumed that there is a 50% probability of choosing either the spiral model or the shrinking encircling mechanism for adjusting whale positions during the optimization process. Let p be the random number in [0, 1] representing the probability, this combined behavior can be mathematically modeled as follows:

$$\overrightarrow{S}(k+1) = \begin{cases} \overrightarrow{S}^*(k) - \overrightarrow{A} \cdot \overrightarrow{D} & \text{if} \quad p < 0.5 \quad (18) \\ \overrightarrow{S}^*(k) + \overrightarrow{D}\, e^{bl} \cos(2\pi l) & \text{if} \quad p \geq 0.5 \quad (19) \end{cases}$$

where b is a constant defining the shape of the logarithmic spiral, and $l \in [-1, 1]$ is a random number.

During the exploration phase, as the whales seek their prey, they employ the methodology outlined in (17) with the condition that $|A| > 1$. This condition is imposed to compel search agents to move a significant distance from a reference whale. Here, $\overrightarrow{S}^*$ is equated to $\overrightarrow{S}_{rand}$, signifying the selection of a random position vector (a random whale) from the existing population. This exploration stage can be

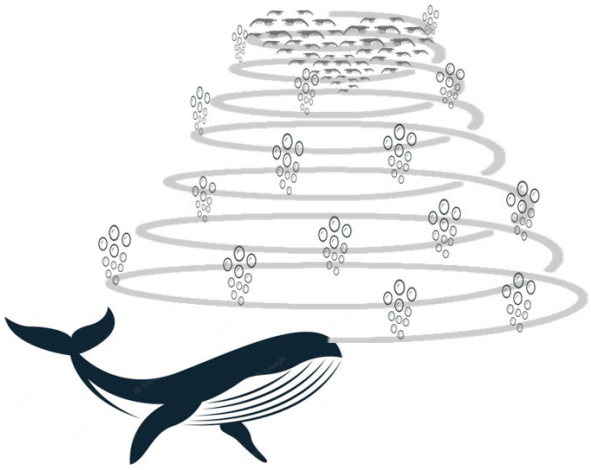

FIGURE 2. Spiral bubble-net foraging behavior of humpback whales.

written as in (20):

$$\begin{cases} \overrightarrow{S}(k+1) = \overrightarrow{S}_{rand}(k) - \overrightarrow{A} \cdot \overrightarrow{D} \\ \overrightarrow{D} = |\overrightarrow{C} \cdot \overrightarrow{S}_{rand}(k) - \overrightarrow{S}(k)| \end{cases} \tag{20}$$

where $\overrightarrow{S}_{rand}$ is the vector representing the position of a random whale in the population.

Algorithm 2 Pseudo-Code of the Standard WOA

```
for i = 1, ..., N do
    Randomly initialize S_i
    Evaluate fitness of each S_i
    Find S*
end for
while k ≤ k_max do
    for i = 1, ..., N do
        Update a, A, p, C and l
        if p < 0.5 then
            if |A| > 1 then Update S(k+1) based on (20)
            else
                Update S(k+1) based on (18)
            end if
        else
            Update S(k+1) based on (19)
        end if
    end for
    Check the fitness of each S_i
    S* ← S_i if f(S_i) < f(S*)
    k++
end while
```

The next subsection provides an explanation of the proposed hybrid PSO-WOA algorithm and the control schemes specifically designed for the BnB system outlined in Section II-A.

D. PROPOSED HYBRID PSO-WOA FOR INTELLIGENT CONTROL DESIGN

In the context of control design via swarm intelligence, a common cost function involves assessing the error between the desired output and the actual output. In this specific scenario, the objective is to regulate the position of the ball at $x = 0$, the time response of x_1 can be simply included in the cost function. In addition, for SF approach where x_2 also needs to be regulated, a generic cost function can be formulated as follows:

$$f(x_1, x_2) = \int_0^{t_f} t(w_1|x_1(t)| + w_2|x_2(t)|)dt \tag{21}$$

where t_f denotes the final simulation time, and w_1, w_2 are weights. To balance the BnB, three distinct cascade control approaches are proposed: PID-PID, PID-SF, and PID-Observer. Fig. 3 provides visual representations of the associated closed-loop systems, with G_b representing the BnB model as outlined in (12), G_m denoting the DC motor model as detailed in (14), and φ_b, φ_c, and φ_m characterizing the position measurement's constraint, beam's physical constraint, and power supply limitation. These nonlinearities are as follows:

$$\varphi_j(u) = \begin{cases} -\epsilon_a & \text{for } u < -\epsilon_a \\ u & \text{for } -\epsilon_a \le u \le \epsilon_a \\ \epsilon_b & \text{for } u > \epsilon_a. \end{cases} \tag{22}$$

where $\epsilon_a = 0.4$m if $j = b$; $\epsilon_a = 0.175$rad if $j = c$; and $\epsilon_a = 5$V if $j = m$. The signals d_0 and $x_1(0)$ represent the external disturbance and initial ball position respectively. The structure of the compensators is described as follows:

$$C_m = K_{pm} + \frac{K_{im}}{s} + \frac{K_{dm}s}{T_f s + 1} \tag{23}$$

$$C_b = K_{pb} + \frac{K_{ib}}{s} + \frac{K_{db}s}{T_f s + 1} \tag{24}$$

$$C_L = K_c(sI - (A_b - L_c C_b - B_b K_c))^{-1} L_c \tag{25}$$

$$K_c = \begin{bmatrix} k_1 & k_2 \end{bmatrix}; \quad L_c = \begin{bmatrix} l_1 & l_2 \end{bmatrix}^T \tag{26}$$

where $A_b \in \mathbb{R}^{2\times2}, B_b \in \mathbb{R}^{2\times1}$ and $C_b \in \mathbb{R}^{1\times2}$ refer to the state-space matrices of the system outlined in (12), $K_c \in \mathbb{R}^{1\times2}$ is the SF gain, $L_c \in \mathbb{R}^{2\times1}$ is the observer's gain, and $T_f \to 0$. Each of these control strategies involves distinct optimization dimensions due to different number of control parameters.

In the case of the PID-PID and PID-Observer structures, wherein x_2 is assumed not accessible and only the output influences the input, w_1 is set to 1 while w_2 is set to 0. Conversely, for the PID-SF structure, where both state variables are regulated, the weights are configured to $w_1 = 0.9$ and $w_2 = 0.1$. In addition, as the system is inherently nonlinear, this study proposes a novel method aimed at mitigating the challenges of encountering local minima and slow convergence when employing WOA and PSO algorithms in optimizing the control parameters. Fig. 4 depicts the suggested hybrid PSO-WOA approach, where the

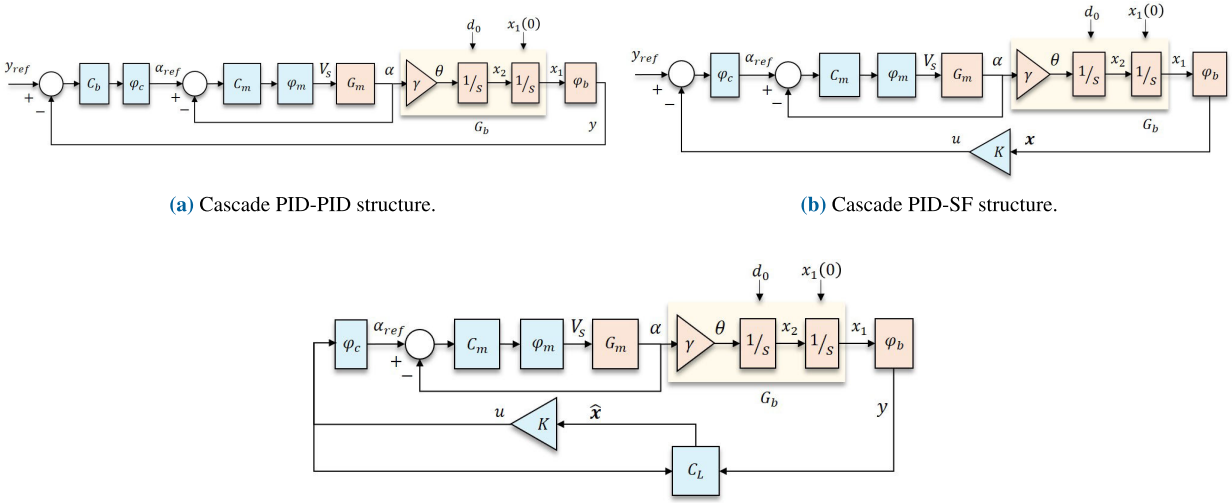

(a) Cascade PID-PID structure.

(b) Cascade PID-SF structure.

(c) Cascade PID-Observer structure where $\hat{x}$ denotes the estimated state vector.

FIGURE 3. Three different control schemes proposed in this study for the BnB system.

initial stage involves setting up populations for both whales and particles. Algorithms 1 and 2 are subsequently executed concurrently. To discern which population is more prone to becoming trapped in local minima, the following definitions are introduced:

$$\begin{aligned}\Delta f_s &= f(S^*(k)) - f(S^*(k-1)),\\ \Delta f_g &= f(g_b(k)) - f(g_b(k-1))\end{aligned} \tag{27}$$

which represent the difference in the cost function between two consecutive iterations. The population that rapidly converges towards the target location initially will be temporarily halted, while the other population continues its search. Once the iteration count reaches three, the performance of the population is assessed through the following equation:

$$\Omega(H) = \frac{1}{3}\sum_{k=h}^{h+2} f(H(k-1)) - f(H(k)) \tag{28}$$

where H can denote either the optimal position of the best whale, i.e., S^*, or the global best position of a particle, i.e., g_b. If $\Omega(H) \leq \epsilon$, where $\epsilon = 0.0001$, it indicates that the population might be stuck in a local minimum. This is because the most recent cost function value exhibits minimal variation compared to the two preceding values. To counteract this, the present position of the population in motion will be passed to the other population that was earlier put on hold. The transition will occur either upon satisfaction of the aforementioned condition or when the iteration count surpasses one-third of the predefined maximum iteration count, denoted as k_{max}. The search activity is then resumed until the iteration count reaches k_{max}. It is worth noting that the proposed hybrid PSO-WOA in this work distinguishes itself from the approaches outlined in [53] and [55] in terms of how and when the whale and particle populations collaborate to exchange information on their positions.

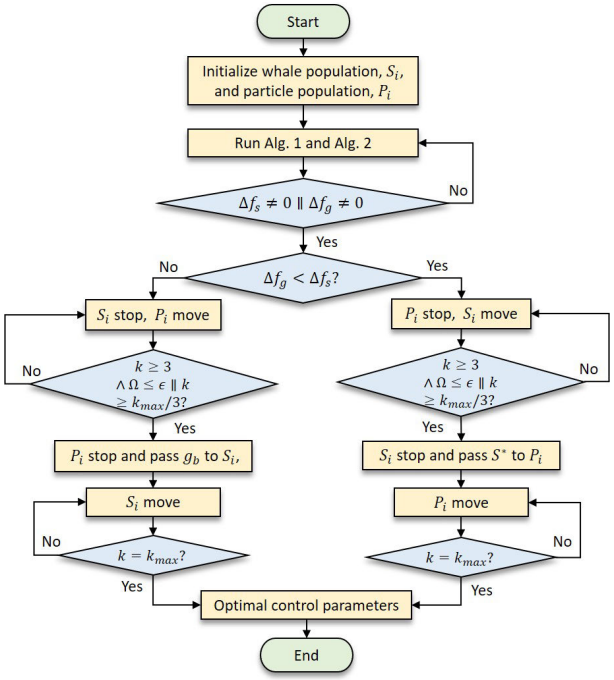

FIGURE 4. Proposed hybrid PSO-WOA algorithm for intelligent control design.

E. PERFORMANCE EVALUATIONS

To evaluate the effectiveness of the proposed hybrid PSO-WOA-optimized compensators, two different scenarios are presented; Scenario 1 and Scenario 2. Both scenarios entail the presence of a non-zero initial ball position along with external disturbances possessing varying amplitudes. For Scenario 1, the initial position is set at $x_1(0) = 20$ cm, while for Scenario 2, it is adjusted to $x_1(0) = -25$ cm.

The external disturbance is introduced as a brief sine wave, simulating a person's contact with the beam. In Scenario 1, this disturbance is applied at $t = 6.2$ s for 0.8 s, with an amplitude ranging from -16.3 cm to 6.35 cm. For Scenario 2, the disturbance is applied at $t = 6.45$ s for 0.6 s, with an amplitude varying between -14.7 cm and 5.7 cm. The main motivation for introducing two distinct scenarios for performance evaluation is to differentiate between Scenario 1, which aims to search for optimal parameters, and Scenario 2, which serves to validate and test the proposed method's generalizability.

To gauge and contrast the performance of the hybrid PSO-WOA approach against its individual components, namely PSO and WOA, as well as conventional control synthesis methods, three performance metrics are employed which are integral time absolute error (ITAE), integral squared error (ISE), and steady-state error (SSE). These metrics are defined as follows:

$$\text{ITAE} = \int_0^{t_f} t|e(t)|dt, \quad \text{ISE} = \int_0^{t_f} e^2(t)dt,$$
$$\text{SSE} = \lim_{t \to t_f} e(t) \tag{29}$$

where $e(t) = x(t)$ since it is a regulator system. ITAE assesses the system's speed of response and error attenuation during transient periods, emphasizing prompt stabilization and minimal oscillations. ISE considers both error magnitude and duration, magnifying significant deviations due to its squared nature. SSE on the other hand measures how accurately the control system can maintain the ball at the desired position without any ongoing corrections. A low SSE is desirable as it means the ball is effectively kept at the setpoint position with minimal deviation. This aspect is critical as in the presence of deliberately introduced external disturbances, it is imperative for the compensator to swiftly attenuate the resulting errors. The following section presents the simulation results and ensuing discussions.

III. RESULTS AND DISCUSSION

This section presents simulation results of the BnB system with the three compensator configurations outlined in the preceding section. The parameter setting for the PSO, WOA and the proposed hybrid PSO-WOA approaches is detailed in Table 2. The bounds of the control parameters are set considering the practical constraints of the BnB, as excessively large parameters could lead the system into unstable regions. In regard to the conventional approaches, the optimization of PID control parameters is executed through the MATLAB PID Tuner, targeting optimal specifications encompassing a faster response time and robust transient behavior. Additionally, for the refinement of SF gains, the conventional LQR approach is employed, which adjusts the gains by minimizing the cost function $J = \int_0^\infty (x^T Q x + u^T R u)dt$ where $Q = I$ and $R = 1$. For the observer, established guidelines are followed for pole placement, ensuring that the poles are positioned ten times faster than the closed-loop poles. The optimized control parameters achieved based on Scenario 1 for the PID-PID, PID-SF, and PID-Observer configurations are documented in Table 3.

For the first control configuration, which is PID-PID, the convergence curve obtained from the proposed hybrid PSO-WOA approach is juxtaposed against the individual components in Fig. 5. Initially at the second iteration, it is evident that Δf_g is smaller than Δf_s, indicating that the particle population primarily drives the search process. Nevertheless, by iteration $k = 7$, the responsibility for the task transitions from g_b to the whale population due to the fulfillment of the condition $k \geq k_{max}/3$. The search process continues until the maximum iteration count is reached. Further analysis of iterations 12 to 20 reveals that the hybrid strategy effectively mitigates the occurrence of local minima issues that are prone to emerge during the PSO search. The effectiveness of the hybrid PSO-WOA is reflected on the time response of the BnB system as depicted in Fig. 6 where it can be clearly seen that x_1 in Fig. 6(a) reaches the equilibrium position notably faster than the rest when the system is initiated with $x_1(0) = 20$ cm, and experiences an external disturbance at $t = 6.2s$. On the contrary, PSO- and WOA-optimized controllers result in relatively larger undershoots. The conventional approach, while not causing undershoot at all, takes the longest time to reach the equilibrium position. Another striking observation is the trajectory of the ball velocity in Fig. 6(b) which reaches the steady-state more rapidly and exhibits reduced oscillations. This highlights the improved capability of the hybrid PSO-WOA technique in maintaining the ball position, in contrast to the individual PSO and WOA methods that continue oscillating to keep the ball at the desired position.

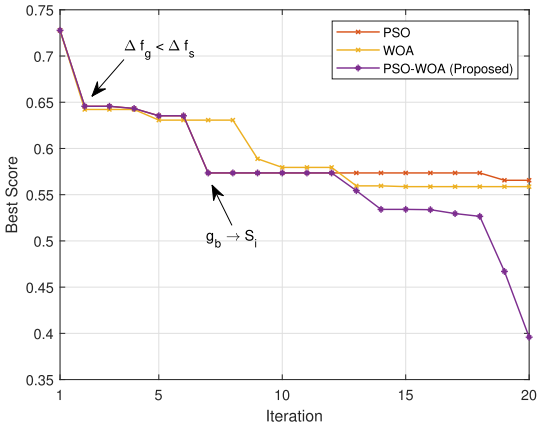

FIGURE 5. Convergence curve comparison between PSO, WOA and the proposed hybrid PSO-WOA for the PID-PID compensator optimization.

Fig. 7 demonstrates the behavior of the BnB system in Scenario 2 where the configurations for $x_1(0)$ and the external disturbance are varied slightly from those in Scenario 1. This variation aims to highlight the methods' ability to perform effectively across different situations and emphasizes their

TABLE 2. Parameter setting for the optimization.

Compensator	N	k_{max}	K_{pm}	K_{im}	K_{dm}	K_{pb}	K_{ib}	K_{db}	k_1	k_2	l_1	l_2
PID-PID	50	20	$[0, 100]$	$[0, 100]$	$[0, 100]$	$[0, 100]$	$[0, 100]$	$[0, 100]$	x	x	x	x
PID-SF	50	20	$[0, 200]$	$[0, 200]$	$[0, 200]$	x	x	x	$[0, 200]$	$[0, 200]$	x	x
PID-Observer	50	20	$[0, 100]$	$[0, 100]$	$[0, 100]$	x	x	x	$[0, 400]$	$[0, 400]$	$[0, 400]$	$[0, 400]$

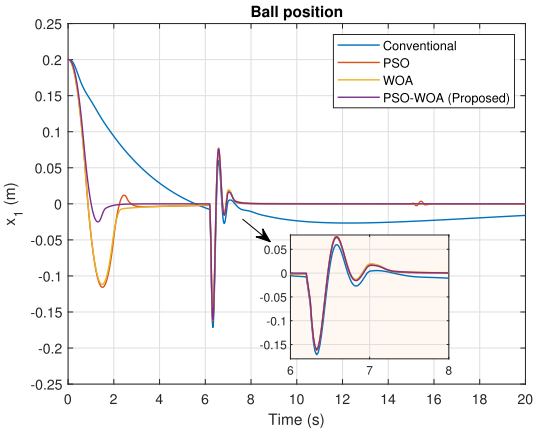

(a) Ball position.

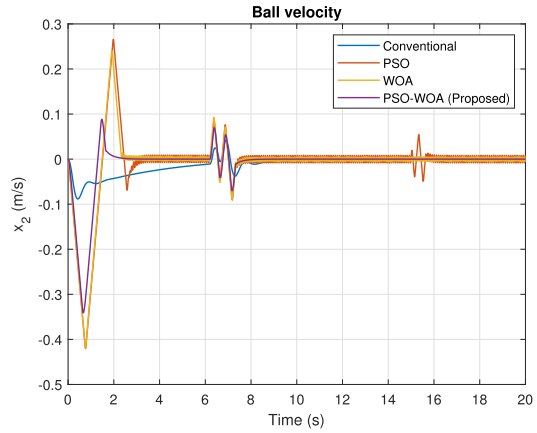

(b) Ball velocity.

FIGURE 6. Comparison of the state trajectories for the BnB with PID-PID compensator for Scenario 1 where $x_1(0) = 20$ cm and d_0 entering the system at $t = 6.2s$.

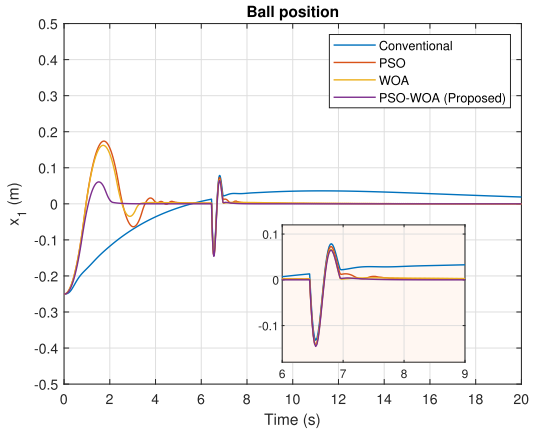

(a) Ball position.

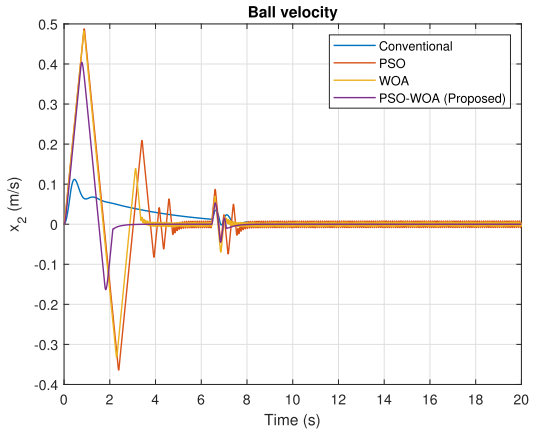

(b) Ball velocity.

FIGURE 7. Comparison of the state trajectories for the BnB with PID-PID compensator for Scenario 2 where $x_1(0) = -25$ cm and d_0 entering the system at $t = 6.45$ s.

generalizability. As can be observed, the proposed hybrid PSO-WOA consistently outperforms the rest in terms of speed and oscillation. Similar to Scenario 1, the controllers based on PSO and WOA exhibit larger overshoots, and the conventional approach requires a longer time to stabilize The corresponding ITAE, ISE, and SSE metrics for each method and scenario are documented in Table 4. It is evident from the table that the hybrid PSO-WOA method consistently attains the lowest values across all categories.

With regard to the PID-SF structure which requires less number of parameters for optimization compared to that of PID-PID structure, Fig. 8 shows the resulting convergence curves, while Fig. 9 and Fig. 10 illustrate the trajectories of the state variables for Scenario 1 and Scenario 2, respectively. Similar to the PID-PID parameter optimization process, the particle population begins the search task in the beginning and then passes the information to the whale population, as visible in Fig. 8. However, the transition takes place slightly earlier as the condition $\Omega \leq \epsilon$ is satisfied at $k = 3$. The minimum cost achieved through the proposed PSO-WOA is lower than those from the PSO and WOA, signifying the effectiveness of the hybrid approach. The impacts of this approach can be observed from the trajectories of x_1 and x_2 in Fig. 9 and Fig. 10 where x_1 reaches the steady-state faster with minimal

TABLE 3. Optimal control parameters for all the three compensator structures.

		Optimal Parameters									
Compensator	**Method**	K_{pm}	K_{im}	K_{dm}	K_{pb}	K_{ib}	K_{db}	k_1	k_2	l_1	l_2
PID-PID	**Conv**	0.088	0.024	0.082	0.540	0.047	1.544	x	x	x	x
	PSO	88.712	44.005	1.439	100.000	22.918	20.077	x	x	x	x
	WOA	86.291	96.210	1.653	82.625	26.055	19.369	x	x	x	x
	PSO-WOA	24.774	11.230	1.456	26.206	0.000	8.876	x	x	x	x
PID-SF	**Conv**	0.0880	0.0237	0.0817	x	x	x	1.4142	0.6609	x	x
	PSO	87.5970	31.6835	3.1766	x	x	x	166.2022	58.8832	x	x
	WOA	177.3879	47.0714	4.9360	x	x	x	175.3394	60.5079	x	x
	PSO-WOA	8.5202	0.0001	0.2090	x	x	x	4.7812	1.4844	x	x
PID-Observer	**Conv**	0.0880	0.0237	0.0817	x	x	x	1.0000	0.5558	35.9850	647.4600
	PSO	61.9691	56.9598	0.0970	x	x	x	326.6874	67.9292	124.9965	267.2354
	WOA	100.0000	100.0000	0.4001	x	x	x	400.0000	95.3928	400.0000	279.1344
	PSO-WOA	100.0000	100.0000	0.3256	x	x	x	400.0000	79.0869	97.1611	400.0000

TABLE 4. Performance evaluations of PID-PID compensator optimized using different methods.

	Scenario 1			Scenario 2			Total		
Method	**ITAE**	**ISE**	**SSE**	**ITAE**	**ISE**	**SSE**	**ITAE**	**ISE**	**SSE**
Conv	4.7008	0.00026	-0.0161	6.1826	0.000357	0.0189	10.884	0.000615	0.00285
PSO	0.5656	1.23E-10	-1.11E-05	0.9236	4.38E-10	2.09E-05	1.4892	5.61E-10	9.80E-06
WOA	0.5587	3.56E-09	-5.96E-05	0.7924	6.26E-09	7.91E-05	1.3511	9.82E-09	1.95E-05
PSO-WOA	**0.3577**	**1.93E-14**	**-1.39E-07**	**0.3595**	**1.76E-14**	**1.33E-07**	**0.7172**	**3.69E-14**	**-6.50E-09**

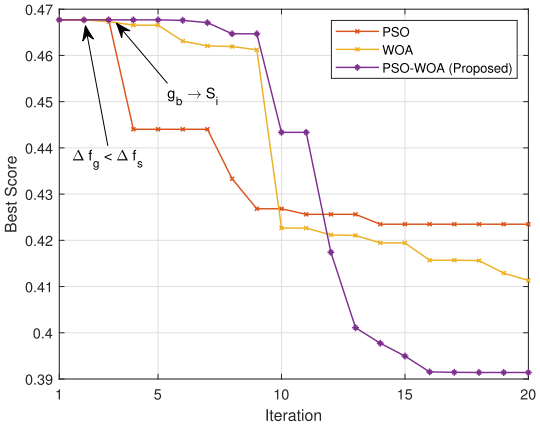

FIGURE 8. Convergence curve comparison between PSO, WOA and the proposed hybrid PSO-WOA for the PID-SF compensator optimization.

oscillations compared to the other methods. The performance of the proposed approach in comparison to the others is documented in Table 5, which also demonstrates reduced ITAE, ISE, and SSE values for each scenario.

The comparison of convergence curves between the hybrid PSO-WOA and its individual components within the PID-Observer structure is presented in Fig. 11. Although the transitional pattern between the particle and whale populations during the search process resembles the patterns observed in the previous two cases, the attained minimum cost through the proposed method only exhibits a marginal reduction in comparison to the costs achieved by the PSO and WOA methods. This trend is also evident in the trajectories of x_1 depicted in Fig. 12. However, the proposed method displays a faster convergence to the steady state as can be seen in Fig. 12(a) with minimal oscillation as displayed in Fig. 12(b) when the system encounters an external disturbance.

The comparison of the state trajectories for the BnB with PID-Observer compensator for Scenario 2 is showcased in Fig.13. In this case, the WOA-optimized controller is able to maintain the performance with a slight undershoot when subjected to disturbance, as depicted in Fig.13(a). In contrast, the conventional PID results exhibit larger oscillations and thus, requires a relatively longer time to drive the ball to the equilibrium position. Another notable observation is the instability induced by the PSO-optimized compensator, where the fluctuation of the ball position increases significantly immediately after the disturbance is imposed. This behavior suggests the occurrence of an overfitting issue during the optimization process, a phenomenon more likely to happen as the dimension of the search space increases. Nevertheless, the proposed hybrid PSO-WOA method is able to sustain its performance while the performance of other methods degrades. The numerical results as recorded in Table 6 underscores the consistent performance of the proposed method across both presented scenarios.

The comprehensive overview of performance, encompassing both the proposed hybrid PSO-WOA method and other

TABLE 5. Performance evaluations of PID-SF compensator optimized using different methods.

	Scenario 1			Scenario 2			Total		
Method	**ITAE**	**ISE**	**SSE**	**ITAE**	**ISE**	**SSE**	**ITAE**	**ISE**	**SSE**
Conv	0.4563	0.0285	-1.30E-06	0.5095	0.0455	9.39E-07	0.9658	0.074	-3.56E-07
PSO	0.4062	0.0240	1.08E-07	0.3906	0.0373	1.02E-07	0.7968	0.06126	2.10E-07
WOA	0.4168	0.0238	4.69E-05	0.4054	0.0371	-2.91E-05	0.8221	0.06094	1.77E-05
PSO-WOA	**0.3732**	**0.0232**	**-2.45E-09**	**0.3608**	**0.0362**	**2.45E-09**	**0.734**	**0.05947**	**7.33E-12**

TABLE 6. Performance evaluations of PID-Observer compensator optimized using different methods.

	Scenario 1			Scenario 2			Total		
Method	**ITAE**	**ISE**	**SSE**	**ITAE**	**ISE**	**SSE**	**ITAE**	**ISE**	**SSE**
Conv	1.7691	0.0600	-2.56E-05	6.5008	0.1341	0.00455	8.2698	0.1941	0.00453
PSO	0.3341	0.0224	3.23E-09	6.1622	0.0529	-2.90E-02	6.4963	0.0753	-0.02897
WOA	0.3387	0.0232	2.27E-09	0.3001	0.0363	1.01E-09	0.6387	0.0595	3.28E-09
PSO-WOA	**0.3334**	**0.0223**	**7.58E-10**	**0.2913**	**0.0350**	**-5.80E-11**	**0.6248**	**0.0573**	**7.0E-10**

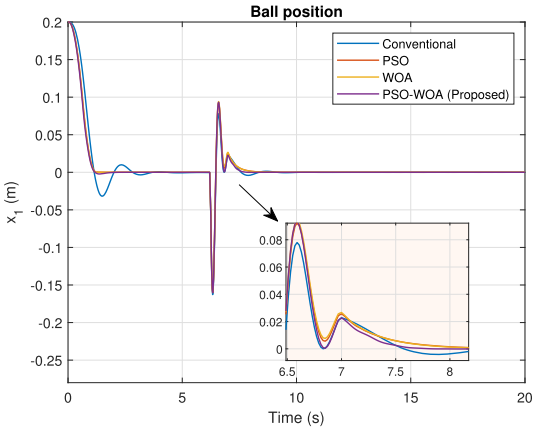

(a) Ball position.

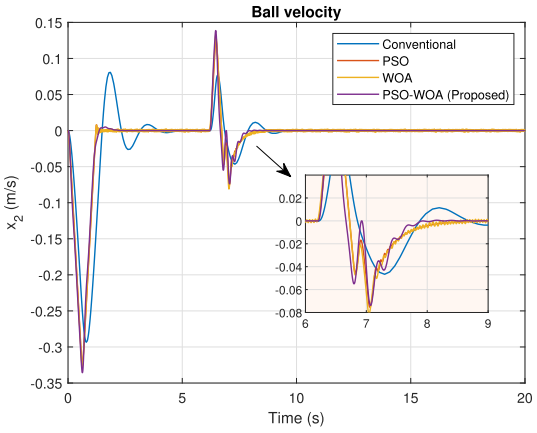

(b) Ball velocity.

FIGURE 9. Comparison of the state trajectories for the BnB with PID-SF compensator for Scenario 1 where $x_1(0) = 20$ cm and d_0 entering the system at $t = 6.2$ s.

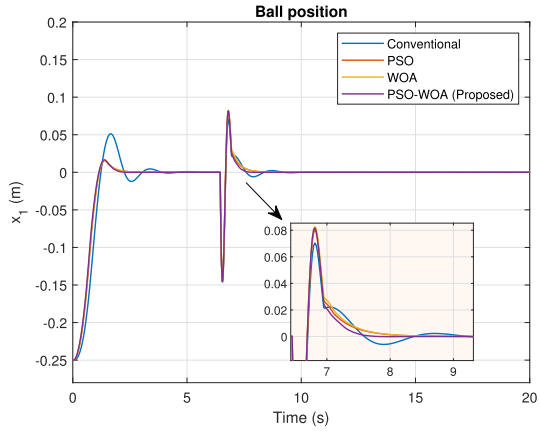

(a) Ball position.

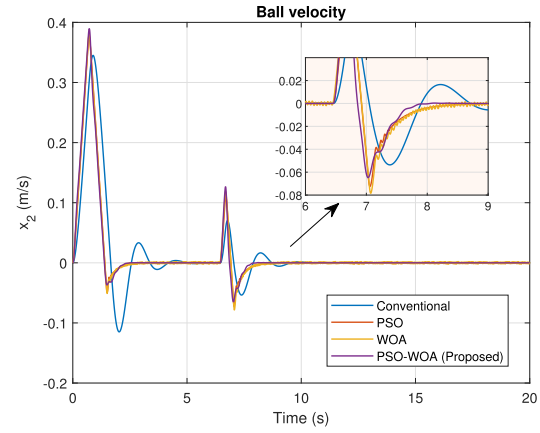

(b) Ball velocity.

FIGURE 10. Comparison of the state trajectories for the BnB with PID-SF compensator for Scenario 2 where $x_1(0) = -25$ cm and d_0 entering the system at $t = 6.45$ s.

techniques for each compensator is summarized in Table 7. The numerical outcomes highlight that the proposed hybrid PSO-WOA approach consistently upholds its performance standards across ITAE, ISE, and SSE metrics, even when

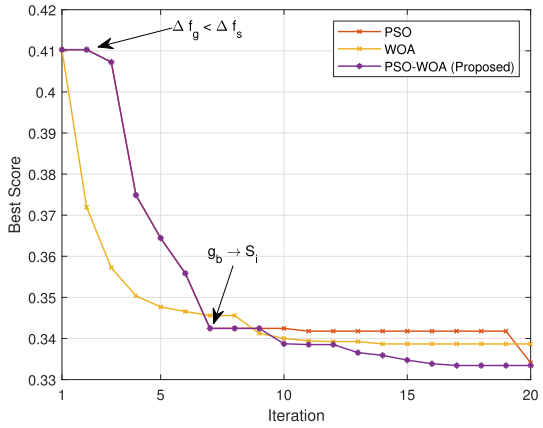

FIGURE 11. Convergence curve comparison between PSO, WOA and the proposed hybrid PSO-WOA for the PID-Observer compensator optimization.

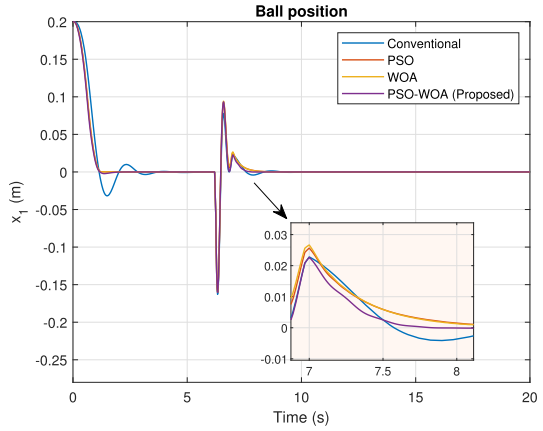

(a) Ball position.

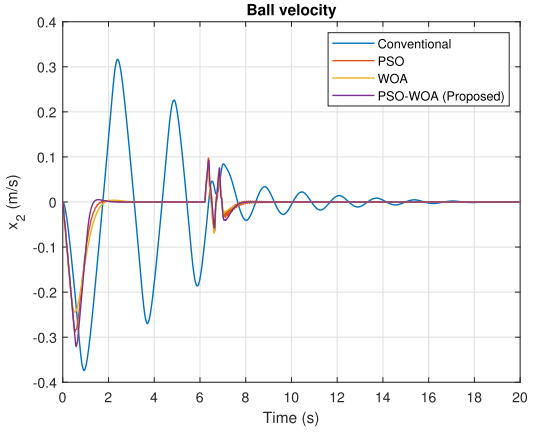

(b) Ball velocity.

FIGURE 12. Comparison of the state trajectories for the BnB with PID-Observer compensator for Scenario 1 where $x_1(0) = 20$ cm and d_0 entering the system at $t = 6.2$ s.

dealing with differing search space dimensions for each compensator. The table reveals that the PID-SF compensator achieves the fastest convergence to zero SSE, primarily due

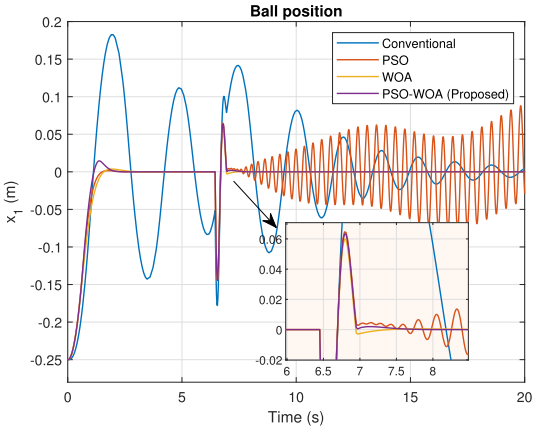

(a) Ball position.

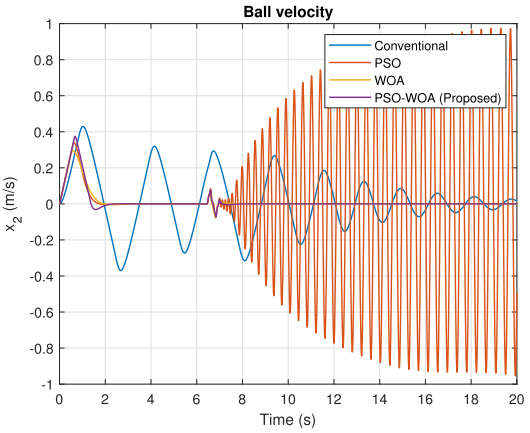

(b) Ball velocity.

FIGURE 13. Comparison of the state trajectories for the BnB with PID-Observer compensator for Scenario 2 where $x_1(0) = -25$ cm and d_0 entering the system at $t = 6.45$ s.

to the feedback scheme being applied to both state variables. In cases where the ball velocity is unobservable, both the PID-PID and PID-Observer can be employed. The PID-PID structure holds an advantage in terms of effectively suppressing the ISE while the PID-Observer compensator exhibits the capability to achieve lower ITAE and SSE values as compared to the PID-PID compensator. However, it is important to highlight that the efficacy of the observer's structure is intricately linked to the precision of the model representing the BnB system. In other words, if the model fails to accurately capture the dynamics of the actual system, the performance is inevitably susceptible to degradation, thus the PID-PID structure can be a better option.

Table 8 quantifies the performance improvement attained by the proposed PSO-WOA method in comparison to the second-best method for each compensator type, based on ITAE, ISE, and SSE. It is evident from the results that the proposed method demonstrates a significant decrease in ITAE by 18.99%, ISE by 35.37%, and SSE by 92.86%. The larger reduction in ISE indicates the efficiency of the proposed

TABLE 7. Summary of performance evaluation for the three types of compensators optimized using different methods.

	Compensator								
	PID-PID			PID-SF			PID-Observer		
Method	ITAE	ISE	SSE	ITAE	ISE	SSE	ITAE	ISE	SSE
Conv	10.884	0.000615	0.00285	0.9658	0.0740	-3.563E-07	8.2698	0.1941	0.00453
PSO	1.4892	5.61E-10	9.8E-06	0.7968	0.06126	2.100E-07	6.4963	0.0753	-0.02897
WOA	1.3511	9.82E-09	1.95E-05	0.8221	0.06094	1.774E-05	0.6387	0.0595	3.28E-09
PSO-WOA	**0.7172**	**3.69E-14**	**-6.5E-09**	**0.7340**	**0.05947**	**7.328E-12**	**0.6248**	**0.0573**	**7.0E-10**

TABLE 8. Performance improvement through the proposed PSO-WOA based on the average ITAE, ISE and SSE across the three compensators.

	Performance Improvement (%)		
Compensator	ITAE	ISE	SSE
PID-PID	46.917	99.993	99.934
PID-SF	7.882	2.412	99.998
PID-Observer	2.176	3.697	78.659
Average (%)	18.99	35.37	92.86

method in minimizing oscillations, while the greater decrease in SSE signifies its ability to swiftly bring the ball to the desired position and maintain it with minimal deviation.

IV. CONCLUSION AND FUTURE WORK

In this study, a novel hybrid PSO-WOA-based intelligent control is introduced to provide an automated search for PID and state feedback control parameters tailored to nonlinear BnB systems. The proposed algorithm is able to strike a good balance between exploring new solutions and exploiting known ones, reducing the risk of getting stuck in local minima or premature convergence. Simulation results consistently highlight the superiority of the hybrid approach over conventional methods and standalone PSO and WOA techniques across diverse scenarios and feedback configurations. This emphasizes the method's effectiveness and generalizability. Notably, the hybrid approach yields a substantial improvement in error metrics, demonstrating an 18.99% reduction in ITAE, a 35.37% reduction in ISE, and a 92.86% reduction in SSE.

While the proposed method demonstrates significant advantages, its practical application to BnB systems may pose challenges due to the need to make several assumptions on ideality a priori. The robustness of the approach under noisy conditions stemming from sensor measurements, and uncertainties due to mechanical motion should be carefully examined as the complexities introduced by these factors could potentially affect the reliability and efficiency of the proposed method. In addressing these challenges, future work could focus on the development of an online adaptive control framework capable of dynamically adjusting controller parameters in real-time. This adaptive framework becomes especially crucial in dealing with significant uncertainties within the system dynamics. The aim is to enhance the adaptability of the proposed approach, allowing it to perform optimally in the face of real-world variations.

Despite these challenges, the observed improvements in error metrics suggest promising directions for future research, particularly in the realm of automated parameter tuning for underactuated nonlinear systems. Addressing the intricacies introduced by sensor noise and mechanical motion will contribute to enhancing the adaptability of the proposed approach. Furthermore, the insights gained from this study have broader applications beyond BnB systems. The automated search for control parameters could extend to various scenarios, such as managing the balance of goods carried by mobile robots, and gyroscopic stabilization systems. This study opens avenues for advancing control strategies in diverse contexts where underactuated nonlinear systems play a pivotal role, emphasizing the potential impact of the proposed hybrid approach on broader technological applications.

ACRONYMS/SYMBOLS

Acronyms/Symbols	Description
BnB	ball and beam
DC	direct current
EMF	back-electromotive force
PD	proportional-derivative
PID	proportional-integral-derivative
LQR	linear quadratic regulator
SF	State Feedback
GA	Genetic Algorithm
ABC	Artificial Bee Colony
BA	Bat Algorithm
PSO	Particle Swarm Optimization
WOA	Whale Optimization Algorithm
ITAE	integral time absolute error
ISE	integral squared error
SSE	steady-state error
$\mathbb{R}^{m\times n}$	$m \times n$ real matrices
Conv	Conventional method

CONFLICT OF INTEREST

The author declares no known competing financial interests or personal relationships that could have appeared to influence the work reported in this paper.

REFERENCES

[1] A. Y. Krasinskii, A. N. Il'ina, and E. M. Krasinskaya, "Modeling of the ball and beam system dynamics as a nonlinear Mechatronic system with geometric constraint," *Vestnik Udmurtskogo Universiteta, Matematika, Mekhanika, Komp'yuternye Nauki*, vol. 27, no. 3, pp. 414–430, Sep. 2017.

[2] C.-L. Shih, J.-H. Hsu, and C.-J. Chang, "Visual feedback balance control of a robot manipulator and ball-beam system," *J. Comput. Commun.*, vol. 5, no. 9, pp. 8–18, 2017. [Online]. Available: https://api.semanticscholar.org/CorpusID:44197243

[3] G. Buza, J. Milton, L. Bencsik, and T. Insperger, "Establishing metrics and control laws for the learning process: Ball and beam balancing," *Biol. Cybern.*, vol. 114, no. 1, pp. 83–93, Feb. 2020.

[4] H. Feng, Y. Xu, and D. Mao, "A novel adaptive balance-drive mechanism for industrial robots using a series elastic actuator," *Int. J. Comput. Integr. Manuf.*, vol. 33, nos. 10–11, pp. 991–1005, Nov. 2020.

[5] S. Monteleone, F. Negrello, G. Grioli, M. G. Catalano, A. Bicchi, and M. Garabini, "A method to benchmark the balance resilience of robots," *Frontiers Robot. AI*, vol. 9, Jan. 2023, Art. no. 817870.

[6] T. C. Lopes, C. G. S. Sikora, R. G. Molina, D. Schibelbain, L. C. A. Rodrigues, and L. Magatão, "Balancing a robotic spot welding manufacturing line: An industrial case study," *Eur. J. Oper. Res.*, vol. 263, no. 3, pp. 1033–1048, Dec. 2017.

[7] L. B. Lau, N. S. Ahmad, and P. Goh, "Self-balancing robot: Modeling and comparative analysis between PID and linear quadratic regulator," *Int. J. Reconfigurable Embedded Syst.*, vol. 12, no. 3, pp. 351–359, Nov. 2023.

[8] M. Velazquez, D. Cruz, S. Garcia, and M. Bandala, "Velocity and motion control of a self-balancing vehicle based on a cascade control strategy," *Int. J. Adv. Robotic Syst.*, vol. 13, no. 3, p. 106, May 2016.

[9] M. M. Kopichev, A. A. Kuznetsov, A. R. Muzalevskiy, and T. L. Rusyaeva, "Ball and beam stabilization laboratory test bench with intellectual control," in *Proc. 23rd Int. Conf. Soft Comput. Meas. (SCM)*, May 2020, pp. 112–116.

[10] N. S. Ahmad, J. H. Teo, and P. Goh, "Gaussian process for a single-channel EEG decoder with inconspicuous stimuli and eyeblinks," *Comput., Mater. Continua*, vol. 73, no. 1, pp. 611–628, 2022.

[11] S. Kuseyri, "Constrained H_∞ control of gyroscopic ship stabilization systems," *Proc. Inst. Mech. Eng., M, J. Eng. Maritime Environ.*, vol. 234, no. 3, pp. 634–641, Aug. 2020.

[12] G. Gembalczyk, P. Domogała, and K. Leśniowski, "Modeling of underactuated ball and beam system—A comparative study," *Actuators*, vol. 12, no. 2, p. 59, Jan. 2023.

[13] I. M. Mehedi, U. M. Al-Saggaf, R. Mansouri, and M. Bettayeb, "Two degrees of freedom fractional controller design: Application to the ball and beam system," *Measurement*, vol. 135, pp. 13–22, Mar. 2019.

[14] A. Rai, S. K. Suman, A. Kumar, and S. Yadav, "Impact of control stability using LQR and pole-placement for ball and beam system," in *Proc. 5th Int. Conf. Intell. Comput. Control Syst. (ICICCS)*, May 2021, pp. 543–547.

[15] Y. Kim, S.-K. Kim, and C. K. Ahn, "Variable cut-off frequency observer-based positioning for ball-beam systems without velocity and current feedback considering actuator dynamics," *IEEE Trans. Circuits Syst. I, Reg. Papers*, vol. 68, no. 1, pp. 396–405, Jan. 2021.

[16] R. Soni and Sathans, "Optimal control of a ball and beam system through LQR and LQG," in *Proc. 2nd Int. Conf. Inventive Syst. Control (ICISC)*, Jan. 2018, pp. 179–184. [Online]. Available: https://api.semanticscholar.org/CorpusID:49539001

[17] S. J. A. Bakar, N. S. Ahmad, and P. Goh, "Improved structured filter design and analysis for perturbed phase-locked loops via sector and H_∞ norm constraints with convex computations," *Comput. Electr. Eng.*, vol. 81, Jan. 2020, Art. no. 106542.

[18] K. Åström and T. Hägglund, *PID Controllers: Theory, Design, and Tuning*. Alexander, NS, USA: International Society of Automation, 1995.

[19] N. S. Ahmad, "Robust stability analysis and improved design of phase-locked loops with non-monotonic nonlinearities: LMI-based approach," *Int. J. Circuit Theory Appl.*, vol. 45, no. 12, pp. 2057–2072, Dec. 2017.

[20] M. Ding, B. Liu, and L. Wang, "Position control for ball and beam system based on active disturbance rejection control," *Syst. Sci. Control Eng.*, vol. 7, no. 1, pp. 97–108, Jan. 2019.

[21] X. Qi, J. Li, Y. Xia, and H. Wan, "On stability for sampled-data nonlinear ADRC-based control system with application to the ball-beam problem," *J. Franklin Inst.*, vol. 355, no. 17, pp. 8537–8553, Nov. 2018.

[22] A. Kharola and P. P. Patil, "Neural fuzzy control of ball and beam system," *Int. J. Energy Optim. Eng.*, vol. 6, no. 2, pp. 64–78, Apr. 2017.

[23] I. Arrouch, N. S. Ahmad, P. Goh, and J. Mohamad-Saleh, "Close proximity time-to-collision prediction for autonomous robot navigation: An exponential GPR approach," *Alexandria Eng. J.*, vol. 61, no. 12, pp. 11171–11183, Dec. 2022.

[24] R. Singh and B. Bhushan, "Real-time control of ball balancer using neural integrated fuzzy controller," *Artif. Intell. Rev.*, vol. 53, no. 1, pp. 351–368, Jan. 2020.

[25] C. H. Goay, N. S. Ahmad, and P. Goh, "Transient simulations of high-speed channels using CNN-LSTM with an adaptive successive halving algorithm for automated hyperparameter optimizations," *IEEE Access*, vol. 9, pp. 127644–127663, 2021.

[26] S.-K. Oh, H.-J. Jang, and W. Pedrycz, "The design of a fuzzy cascade controller for ball and beam system: A study in optimization with the use of parallel genetic algorithms," *Eng. Appl. Artif. Intell.*, vol. 22, no. 2, pp. 261–271, Mar. 2009.

[27] M. Amjad, M. I. Kashif, S. S. Abdullah, and Z. Shareef, "Fuzzy logic control of ball and beam system," in *Proc. 2nd Int. Conf. Educ. Technol. Comput.*, vol. 3, Jun. 2010, pp. 489–493.

[28] N. S. Ahmad, "Robust H_∞-fuzzy logic control for enhanced tracking performance of a wheeled mobile robot in the presence of uncertain nonlinear perturbations," *Sensors*, vol. 20, no. 13, p. 3673, Jun. 2020.

[29] M. J. Mahmoodabadi and N. Danesh, "Gravitational search algorithm-based fuzzy control for a nonlinear ball and beam system," *J. Control Decis.*, vol. 5, no. 3, pp. 229–240, Jul. 2018.

[30] A. Q. Al-Dujaili, A. J. Humaidi, D. A. Pereira, and I. K. Ibraheem, "Adaptive backstepping control design for ball and beam system," *Int. Rev. Appl. Sci. Eng.*, vol. 12, no. 3, pp. 211–221, Jul. 2021.

[31] S. Yao, X. Liu, Y. Zhang, and Z. Cui, "Research on solving nonlinear problem of ball and beam system by introducing detail-reward function," *Symmetry*, vol. 14, no. 9, p. 1883, Sep. 2022. [Online]. Available: https://www.mdpi.com/2073-8994/14/9/1883

[32] O. D. Montoya, W. Gil-González, and C. Ramírez-Vanegas, "Discrete-inverse optimal control applied to the ball and beam dynamical system: A passivity-based control approach," *Symmetry*, vol. 12, no. 8, p. 1359, Aug. 2020.

[33] M. Vásquez, J. Yanascual, M. Herrera, A. Prado, and O. Camacho, "A hybrid sliding mode control based on a nonlinear PID surface for nonlinear chemical processes," *Eng. Sci. Technol., Int. J.*, vol. 40, Apr. 2023, Art. no. 101361.

[34] M. R. Rosa, M. Z. Romdlony, and B. R. Trilaksono, "The ball and beam system: Cascaded LQR-FLC design and implementation," *Int. J. Control, Autom. Syst.*, vol. 21, no. 1, pp. 201–207, Jan. 2023.

[35] A. Umar, M. B. Mu'azu, Z. Haruna, O.-O. Ajayi, N. S. Usman, O. J. Oghenetega, and A. D. Adekale, "Performance comparison of the ball and beam system using linear quadratic regulator controller," in *PID Control for Linear and Nonlinear Industrial Processes*, M. Shamsuzzoha and G. L. Raja, Eds. Rijeka, Croatia: IntechOpen, 2023, ch. 7.

[36] P. V. M. Maalini, G. Prabhakar, and S. Selvaperumal, "Modelling and control of ball and beam system using PID controller," in *Proc. Int. Conf. Adv. Commun. Control Comput. Technol. (ICACCCT)*, May 2016, pp. 322–326.

[37] S. J. A. Bakar, K. J-Shenn, P. Goh, and N. S. Ahmad, "Development of magnetic levitation system with position and orientation control," *Int. J. Reconfigurable Embedded Syst.*, vol. 12, no. 2, pp. 287–296, Jul. 2023.

[38] M. F. Rahmat, H. Wahid, and N. A. Wahab, "Application of intelligent controller in a ball and beam control system," *Int. J. Smart Sens. Intell. Syst.*, vol. 3, no. 1, pp. 45–60, Jan. 2010.

[39] S. Ekinci, B. Hekimoğlu, and D. Izci, "Opposition based Henry gas solubility optimization as a novel algorithm for PID control of DC motor," *Eng. Sci. Technol., Int. J.*, vol. 24, no. 2, pp. 331–342, Apr. 2021.

[40] A. Y. Jaen-Cuellar, R. D. J. Romero-Troncoso, L. Morales-Velazquez, and R. A. Osornio-Rios, "PID-controller tuning optimization with genetic algorithms in servo systems," *Int. J. Adv. Robotic Syst.*, vol. 10, no. 9, p. 324, Sep. 2013.

[41] B. Meenakshipriya and K. Kalpana, "Modelling and control of ball and beam system using Coefficient Diagram Method (CDM) based PID controller," *IFAC Proc. Volumes*, vol. 47, no. 1, pp. 620–626, 2014.

[42] M. Keshmiri, A. F. Jahromi, A. Mohebbi, M. H. Amoozgar, and W.-F. Xie, "Modeling and control of ball and beam system using model based and non-model based control approaches," *Int. J. Smart Sens. Intell. Syst.*, vol. 5, no. 1, pp. 14–35, Jan. 2012.

[43] R. M. Kagami, G. K. da Costa, T. S. Uhlmann, L. A. Mendes, and R. Z. Freire, "A generic WebLab control tuning experience using the ball and beam process and multiobjective optimization approach," *Information*, vol. 11, no. 3, p. 132, Feb. 2020.
[44] A. Loganathan and N. S. Ahmad, "A systematic review on recent advances in autonomous mobile robot navigation," *Eng. Sci. Technol., Int. J.*, vol. 40, Apr. 2023, Art. no. 101343.
[45] M. Y. Coskun and M. Itik, "Intelligent PID control of an industrial electro-hydraulic system," *ISA Trans.*, vol. 139, pp. 484–498, Aug. 2023.
[46] P. Ouyang and V. Pano, "Comparative study of DE, PSO and GA for position domain PID controller tuning," *Algorithms*, vol. 8, no. 3, pp. 697–711, Aug. 2015. [Online]. Available: https://www.mdpi.com/1999-4893/8/3/697
[47] A. T. Azar, N. Ali, S. Makarem, M. K. Diab, and H. H. Ammar, "Design and implementation of a ball and beam PID control system based on Metaheuristic techniques," in *Proc. Int. Conf. Adv. Intell. Syst. Inform.*, A. E. Hassanien, K. Shaalan, and M. F. Tolba, Eds. Cham, Switzerland: Springer, 2020, pp. 313–325.
[48] E. S. Ghith and F. A. A. Tolba, "Real-time implementation of tuning PID controller based on whale optimization algorithm for micro-robotics system," in *Proc. 14th Int. Conf. Comput. Autom. Eng. (ICCAE)*, Mar. 2022, pp. 103–109.
[49] V. Estrela, N. Razmjooy, Z. Vahedi, A. Monteiro, and R. França, "Speed control of a DC motor using PID controller based on improved whale optimization algorithm," *Metaheuristics Optim. Comput. Elect. Eng.*, vol. 696, pp. 153–167, Nov. 2020.
[50] F. Loucif, S. Kechida, and A. Sebbagh, "Whale optimizer algorithm to tune PID controller for the trajectory tracking control of robot manipulator," *J. Brazilian Soc. Mech. Sci. Eng.*, vol. 42, no. 1, pp. 1–11, Jan. 2020.
[51] V. Steffen, "Particle swarm optimization with a simplex strategy to avoid getting stuck on local optimum," *AI, Comput. Sci. Robot. Technol.*, vol. 2022, pp. 1–40, Oct. 2022.
[52] S. B. Joseph, E. G. Dada, A. Abidemi, D. O. Oyewola, and B. M. Khammas, "Metaheuristic algorithms for PID controller parameters tuning: Review, approaches and open problems," *Heliyon*, vol. 8, no. 5, May 2022, Art. no. e09399.
[53] H.-P. Hsu and C.-N. Wang, "Hybridizing whale optimization algorithm with particle swarm optimization for scheduling a dual-command storage/retrieval machine," *IEEE Access*, vol. 11, pp. 21264–21282, 2023.
[54] V. Srivastava, S. Srivastava, H. Malik, G. Chaudhary, and S. Srivastava, "Hybrid optimization based PID control of ball and beam system," *J. Intell. Fuzzy Syst.*, vol. 42, no. 2, pp. 919–928, Jan. 2022.
[55] I. Trivedi, P. Jangir, A. Kumar, N. Jangir, and R. Totlani, "A novel hybrid PSO-WOA algorithm for global numerical functions optimization," *Adv. Comput. Comput. Sci.*, vol. 554, pp. 53–60, Sep. 2017.
[56] K. Nowopolski, "Ball-and-beam laboratory system controlled by Simulink model through dedicated microcontrolled-MATLAB data exchange protocol," *Comput. Appl. Electr. Eng.*, vol. 11, pp. 310–320, 2013. [Online]. Available: https://yadda.icm.edu.pl/baztech/element/bwmeta1.element.baztechde01a646-1528-420f-8f26-167a80e8c197?q=bwmeta1.element.baztech-2108ab3f-936c-4c0aadb5-32aa63a7a42b;30&qt=CHILDREN-STATELESS
[57] N. H. Jo and J. H. Seo, "A state observer for nonlinear systems and its application to ball and beam system," *IEEE Trans. Autom. Control*, vol. 45, no. 5, pp. 968–973, May 2000.
[58] N. S. Ahmad, J. Carrasco, and W. P. Heath, "LMI searches for discrete-time Zames–Falb multipliers," in *Proc. 52nd IEEE Conf. Decis. Control*, Dec. 2013, pp. 5258–5263.
[59] C. Pozna and R.-E. Precup, "An approach to the design of nonlinear state-space control systems," *Stud. Informat. Control*, vol. 27, no. 1, pp. 5–14, Mar. 2018.
[60] R. Eberhart and J. Kennedy, "A new optimizer using particle swarm theory," in *Proc. 6th Int. Symp. Micro Mach. Human Sci.*, Oct. 1995, pp. 39–43.
[61] S. Mirjalili and A. Lewis, "The whale optimization algorithm," *Adv. Eng. Softw.*, vol. 95, pp. 51–67, May 2016.

NUR SYAZREEN AHMAD (Member, IEEE) received the B.Eng. degree in electrical and electronic engineering and the Ph.D. degree in control systems from The University of Manchester, U.K. She is currently an Associate Professor with the School of Electrical and Electronic Engineering, University Sains Malaysia (USM), specializing in embedded control systems, sensor networks, and mobile robotics. Her main research interests include autonomous mobile robots, with a particular focus on sensing, identification, intelligent control, and indoor navigation. She is a member of IEEE Young Professional and Control System Societies and has served as a reviewer for several high-impact journals within her field.